

URTeC: 3114

Evaluating Primary-Infill Well Performance After Frac Mitigation Using Fracture-Type Diagnostics in the Midland Basin Wolfcamp Shale

Yvonne Scherz, P.E.*¹, Yogashri Pradhan, P.E.¹, Michael Rainbolt, P.E.², Thomas Johnston³ 1. Endeavor Energy Resources, L.P., 2. Abra Controls Corporation, 3. ShearFRAC Group, LLC.

Copyright 2020, Unconventional Resources Technology Conference (URTeC) DOI 10.15530/urtec-2020-3114

This paper was prepared for presentation at the Unconventional Resources Technology Conference held in Austin, Texas, USA, 20-22 July 2020.

The URTeC Technical Program Committee accepted this presentation on the basis of information contained in an abstract submitted by the author(s). The contents of this paper have not been reviewed by URTeC and URTeC does not warrant the accuracy, reliability, or timeliness of any information herein. All information is the responsibility of, and, is subject to corrections by the author(s). Any person or entity that relies on any information obtained from this paper does so at their own risk. The information herein does not necessarily reflect any position of URTeC. Any reproduction, distribution, or storage of any part of this paper by anyone other than the author without the written consent of URTeC is prohibited.

Abstract

There are many recent efforts on fracture mitigation to ensure competitive infill wells. While operators are trying to overcome asymmetrical fractures caused by existing primary wells, there is also a continuous effort to evaluate the quality of the fracture surface area for the infill wells. SPE 199686-MS covered passive frac mitigation using water to pre-load two Upper and two Lower Wolfcamp primary wells in the Midland Basin. The goal of the study is to determine the success of the pre-load trial by studying the infill well created fractures. We accomplished this using diagnostic plots such as Volume to First Response (VFR), Instantaneous Shut-in Pressure (ISIP), Rate Transient Analysis (RTA) and by characterizing the number of fractures using fracture-type diagnostics. Shear fractures maximize the fracture surface area (FSA) of the well; tensile fractures have limited FSA. Tensile fractures are also a characteristic of asymmetrical fractures, and these, are the types of fractures found in well-to-well communication.

The passive frac mitigation method and initial production results are covered in SPE 199686-MS. The team recorded second by second pressure data with pre-loaded and offset shut-in primary and infill wells. Time was synchronized to absolute reference time to properly assign the origin of fracture driven interactions (FDIs) as they occurred. By use of frac treatment pressure data, the team was able to determine the number of shear and tensile fractures. Then during flowback, the team compared production results per well with the estimated number of resulting shear fractures. For other co-developed infill wells in the same bench, the team also compared the number of shear fractures to determine if frac mitigation technique of pre-loading aided in maximizing the number of shear fractures.

The team found correlations between the number of tensile fractures measured and location of FDIs. VFR plots confirmed frac-frac connections during the higher-magnitude FDIs. Most interestingly, “low” FDI pressures of 50 -100 psi size were responsible for most of the frac to frac communication. RTA linear flow parameter (LFP), also known as $A_c\sqrt{k}$, showed correlation with both VFR and the number of shear fractures.

Incorporating the fracture type in evaluating fracture mitigation techniques provides another dimension to understanding and determining success of the infill well. In our study, frac mitigation using pre-load is not just preventing asymmetrical fractures, but also aiding the maximum FSA created. Production and RTA results confirm that the number of shear fractures and differentiating fracture types are valid metrics. Targeting the right type of fracture during completion when making “on-the-fly” completion modifications may be an important role in frac mitigation.

Introduction

The rising inventory of drilled but uncompleted (DUC) wells make the understanding of FDI mitigation critical. In this study, we needed to evaluate our first order infill completion quality after pre-loading the primary wells in a frac mitigation trial (Scherz, et al. 2020.) The aim is to quantitatively characterize the infill completion by the type and number of fractures created along the wellbore. If the pre-loading were successful at mitigating asymmetrical fractures, the first order infill would have shear and tensile fractures comparable to the other co-developed infill wells. A patented software algorithm that can distinguish frac treatment pressure into tensile or shear fractures was employed. Tensile fractures have limited FSA and are the type of fracture found in the well-to-well communication. Shear fractures, on the other hand, maximize the FSA of the infill well which leads to increased early production. **FIGURE 1** shows a sketch rendering of tensile vs. shear fractures.

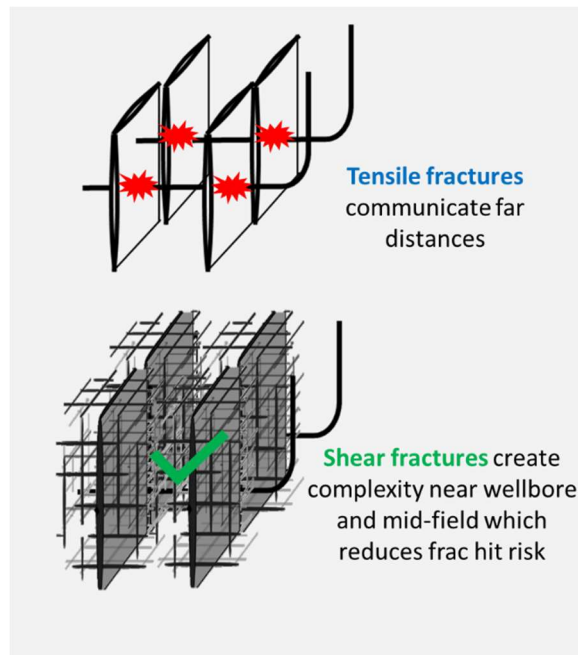


Figure 1—Tensile fractures vs. shear fractures

Our study also analyzed the completion stages with diagnostic tools such as VFR plots introduced by Haustveit e.al.(2019), and ISIP plots. Finally, we used RTA to further appraise the pre-load trial.

Background

In 2019, we trialed a passive frac mitigation technique of pre-loading the primary well with water. We reported the method and initial observations in SPE 199686-MS (Scherz, et al., 2020). For reference, **FIGURE 2 and FIGURE 3** show the relative location of the primary, infills, and volumes of water injected.

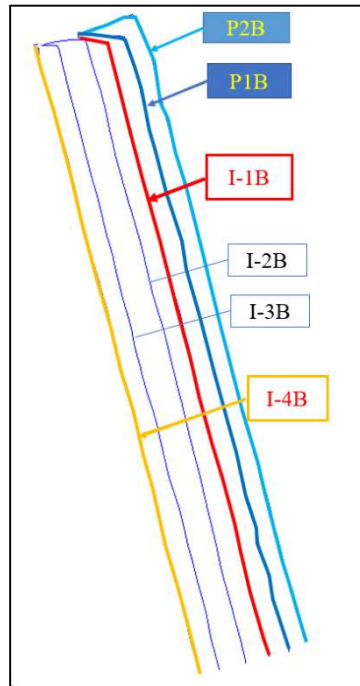


Figure 3—Plan view of primary and infill wells

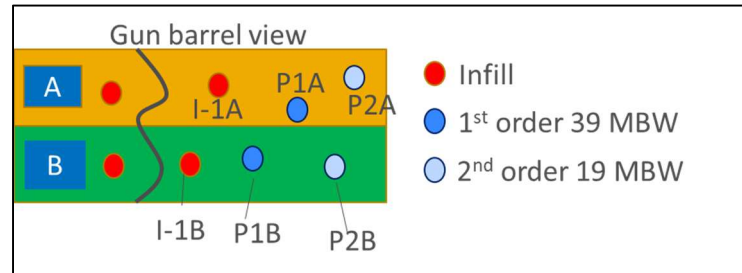


Figure 2—Gun barrel view of wells

Geology

Physical experiments have been designed and performed to empirically show how fractures develop in unconventional reservoirs (Suarez-Rivera, et al., 2013). Unconventional reservoirs are organic-rich, fine-grained, and highly laminated. Low viscosity slickwater enters the laminations, shearing the horizontal planes; and creates small, vertical tensile fractures, spaced at the thickness of the lamination (Gross, et al., 1995). Fine-grained proppant is drawn into small fractures via the Bernoulli principle, converting hydraulic pressure to stress and diverting fluid to further fracture the rock. Taking advantage of the rock's tectonic fabric increases the density of fractures created, improving recovery efficiency and productivity.

Improving recovery efficiency and productivity from fractures can be aided during the completion operations by using pressure measured every second. Microseismic events can be produced at the end of the stage, allowing a first take on the fracture dimensions created before the next stage has begun. New technologies are also capable of using offset pressure gauges and inter-stage measurements to give a good determination of fracture dimension. However, none of these technologies allow operators to make intra-stage changes and see how it affects the completion effectiveness. The geology changes from stage-to-stage, and even during the stage from near- to far-wellbore. To adapt and make appropriate changes, it is essential to determine the numbers and types of fractures occurring every second to further improve completion effectiveness.

Methodology

Fracture Type Identification

The only true real-time measurement of derived completion effectiveness is from the treatment pressure taken at the wellhead. The pumped fluid has a direct hydraulic connection to the fracture tips. The incompressible nature of water means that any fluctuations in the surface pressure measurement must be either mechanical or geological. The geological component can be extracted from the pressure signal using neural nets and artificial intelligence (United States of America Patent No. 16/190,088, 2019). Neural nets allow the pressure signal to be separated between tensile and shear fractures.

FDI Measurement and Volume to First Response Measurement

First, a refresher of FDI KEY DATA POINTS. **FIGURE 4** shows one stage of a treatment well, with the surface treatment pressure on the left y-axis and the observation well pressure on the right y-axis. The red

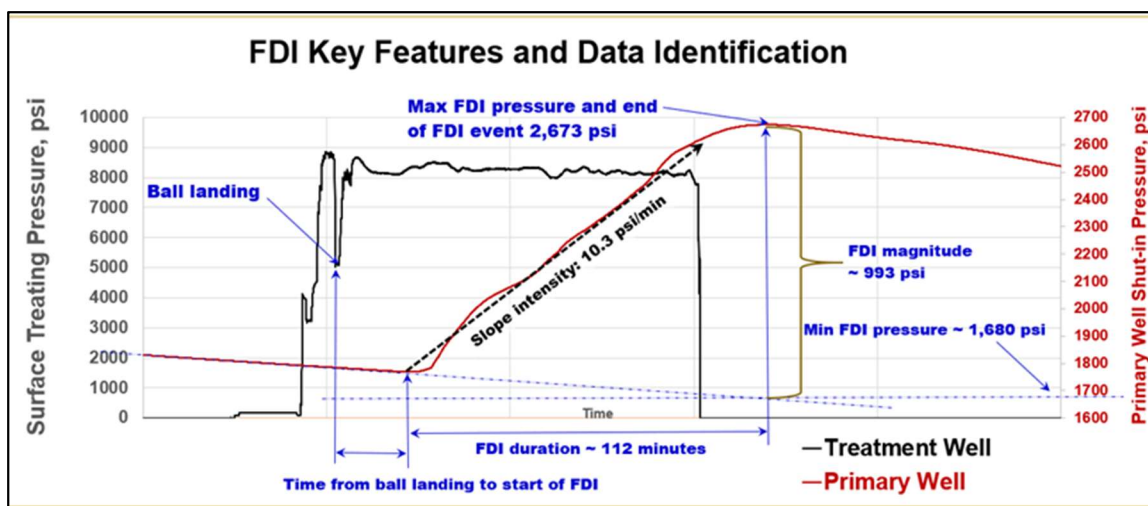


Figure 4—FDI analysis

line is the observation well pressure as it experiences the FDI. The FDI starting time is captured when the natural fall-off pressure trend is interrupted by early communication with the fracturing operations. In this case, we have labeled beginning of the FDI as “fracture shadowing” (Daneshy, A. 2018).

Subsequently, the fracturing shadowing is followed by fracture to fracture hydraulic connection (fluid exchanged). This is marked in Fig.4 at the beginning of the FDI Event Slope Intensity line. The ending FDI time and maximum FDI pressure is captured where the FDI slope intensity becomes zero. Delta FDI time is measured from the time fracture shadowing begins until max FDI pressure occurs. Minimum FDI pressure is the projected pressure from the prior fall-off trend, measured at time of the current maximum FDI pressure. It is NOT equal to the pressure at the start of fracture shadowing. These measurements and recordings are made for each stage. For this job, we had four wells with about 69 stages each or 276 stages to analyze.

We analyzed the VFR similarly, stage by stage using time-synchronized pressure measurements. **FIGURE 5** shows an example of the mechanics of determining the VFR. One stage of a treatment well is

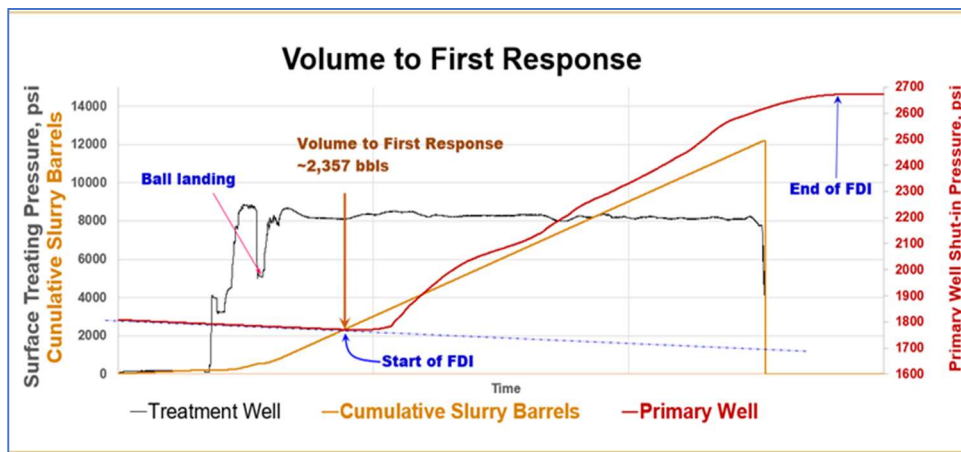


Figure 5–VFR Analysis

shown with the surface treatment pressure on the left, y-axis. The red line is the observation well pressure (right y-axis) as it realizes the FDI. The time when the ball lands is recorded. The time to first response is recorded when the pressure slope of the observation well changes. The total volume pumped to this time is the VFR. If the pressure point of change is difficult to determine, the first derivative may be helpful to pinpoint the pressure change.

Results

Fracture Driven Interactions Observed

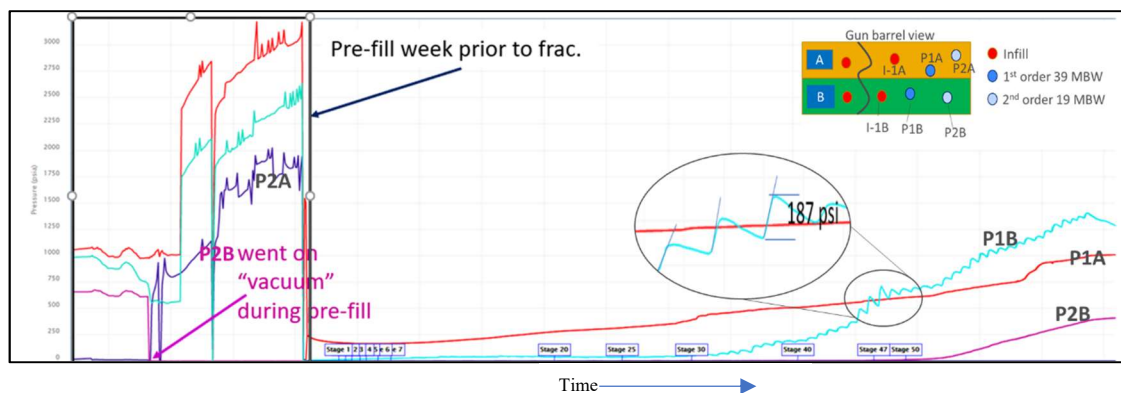


Figure 6–Preload mitigation trial: pressure observations at primary wells

FIGURE 6 shows the pre-load pressures and FDIs observed in the primary wells during frac operations. In SPE 199686, we used this pressure vs. time graph to make a quick observation that only well P1B had experienced any FDIs and that that the pressure magnitudes were relatively smaller than what had been observed in other nearby trials. The updated, stage by stage analysis of the P1B well pressures identified 38 FDIs, 34 frac to frac and 4 fracture shadowing. Another 14 pressure increases were not considered FDIs.

One of our key performance indicators (KPI) for a successful trial was that the FDIs would be less than the magnitude of 100 psi, an educated-guess benchmark set by the team. Three of the 38 frac-to frac FDIs exceeded 100 psi but the question remained whether the pre-load had been effective in stopping or lessening the incursion of frac fluid into the primary well.

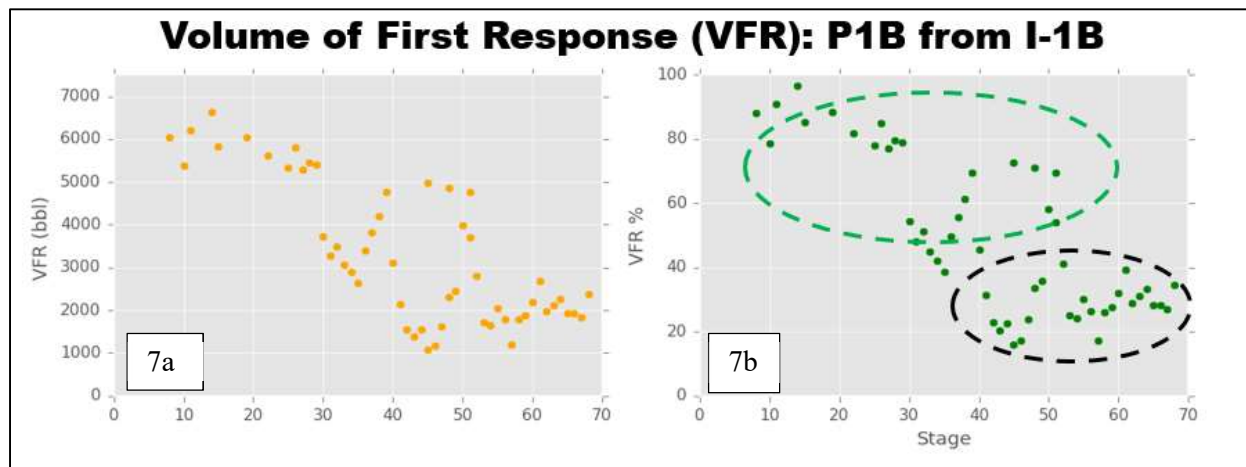


Figure 7–VFR analysis: Well P-1B from I-1B

We turn to a concept introduced by Haustveit e.al.(2019), the Volume of First Response (VFR). This analysis requires time synchronized pressure in both the primary and the infill or active frac well. The VFR was extracted for each stage in the infill-to-primary pair. The VFR for the P1B to I-1B pair presented in **FIGURE 7 (7a)** shows the volume of frac fluid pumped into the infill I-1B until a pressure response was seen in the P1B. **FIGURE 7 (7b)** shows VFR expressed as a percent of the total stage volume pumped. The significance of this information is that it quantitatively shows the volume of fluid used to create new producing fractures for the infill well. The more volume, the higher the FSA created, the better. Small volumes would indicate that the fluid found a connection to the existing well’s fractures quickly leading to inefficient fracturing of the formation around the infill well. Figure 7b, top circled data, indicates that during the first 50 stages, most of the stimulation fluids did not communicate with the primary well. But, from stages 40 forward, less than 40% of the frac fluid effectively stayed in the infill (lower circle in Fig.7b). Indeed, this data correlates with the observed pressure responses (Fig. 6) when the FDI magnitudes start increasing. VFR plots confirmed frac-frac connections during the higher-magnitude FDIs specifically at the three highest magnitudes in stages 45 to 47.

FIGURE 8 shows the magnitude of the FDIs by stage. Most interestingly, “low” FDI pressures of 50 -100 psi size (lower circle in Fig. 8) were responsible for most of the frac-fluid communication from the VFR analysis shown in the corresponding stages in Fig. 7b.

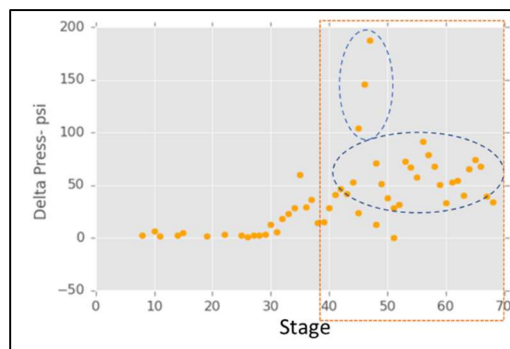


Figure 8 Fracture Driven Interaction Pressure Magnitude by Stage

When the values of FDI magnitude, event to FDI time and percent VFR are graphed together by stage, a strong correlation of VFR and event to FDI time is detected. An inverse correlation of VFR to FDI magnitude can also be observed in **FIGURE 9**.

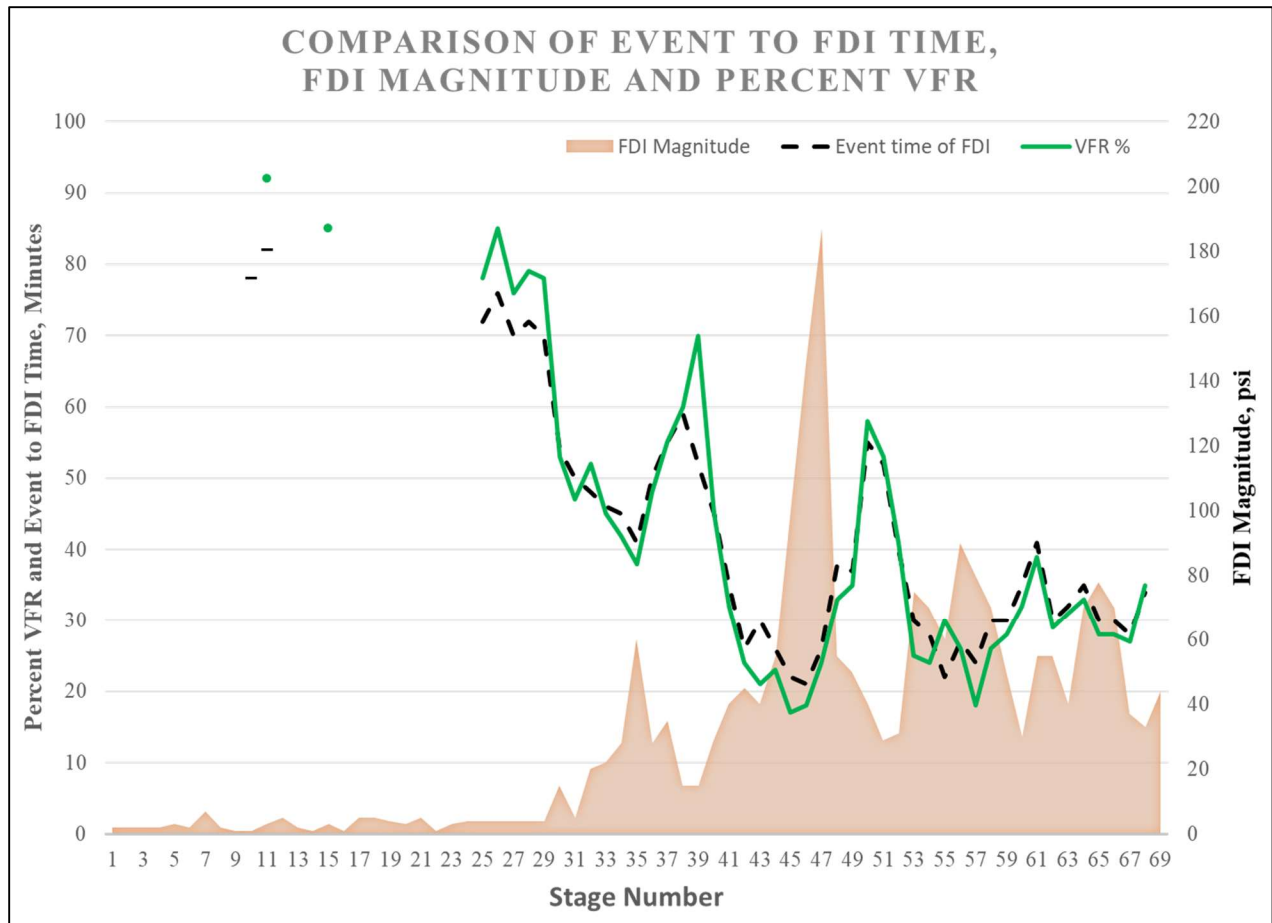


Figure 9–Well I-1B and P1B: Comparison of event to FDI time, FDI magnitude and percent VFR by stage

This graph illustrates that a fast pressure response at the observation well may indicate a fracture to fracture connection which in turn means that the volume of first response will be small. These two parameters at their lowest values yield the highest FDI magnitude value. When the observation well, P1B, experienced stress-shadow pressure magnitudes (under 20 psi), the VFR rose above 50% in infill well I-1B.

ISIP pressures per stage in **FIGURE 10** show an increasing trend with each stage. This is interpreted as stress shadowing and could also indicate height growth containment. Stress shadowing occurs as a result of created fractures competing for width. When this happens, created fractures will follow the path of least resistance which could cause fractures to divert and grow up or down toward the zone of lowest

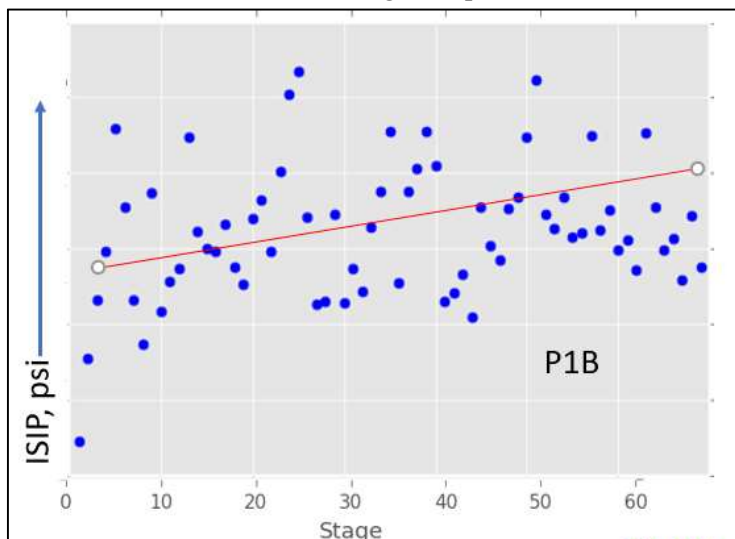


Figure 10–ISIP by stage

stress. Increasing stress can also result in less fracture width or some of the clusters to shut down early (coalescence or “super clusters”), Scherz et al. (2019). This in turn causes the VFR to decrease which is a sign of reduced fracture efficiency. Reduced fracture efficiency, or lack of containment from stages 40 and onward, contributed to low VFR in the latter, heel, stages (Fig. 7b).

The time-synchronized pressure data was then processed by a proprietary technology that differentiates between tensile and shear fractures. We compared the first order infill well with the other infills to see if the infill suffered any degradation from the depleted primary fractures. If the pre-load were effective, our hypothesis was that few tensile fractures would be generated in the first order infill, or that it would be comparable to the other co-developed infill wells. A gun barrel view of the wells presented in **FIGURE 11** shows the position of P1B and I-1B and the other co-developed infills in the Middle Wolfcamp bench. For brevity, we present the fracture identification results of the I-1B and show the I-4B as a representative example of the co-developed infill wells.

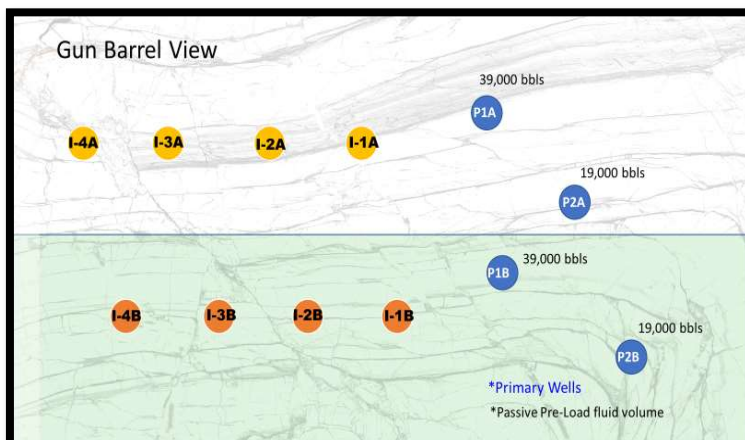


Figure 11–Gun barrel view of primary and infill wells

FIGURE 12 displays the number of shear fracture and tensile fractures detected at each stage in the infill well I-1B. In this well, more shear fractures than tensile fractures were created, generating higher FSA. By comparison, the I-4B (**FIGURE 13**) which is unbounded on the west side (Fig.11) had a similar amount of tensile fractures but a much smaller count of shear fractures. Greater shear fracturing occurred in the first order infill, well I-1B, as the pre-loading (of P1B) lubricated the rock fabric, resulting in lower stress for fracture initiation. High shear fracture counts in I-1B show efficient fracturing of the surrounding formation. Low shear fracture counts in I-4B suggest room to more efficiently fracture the near-wellbore region to improve productivity.

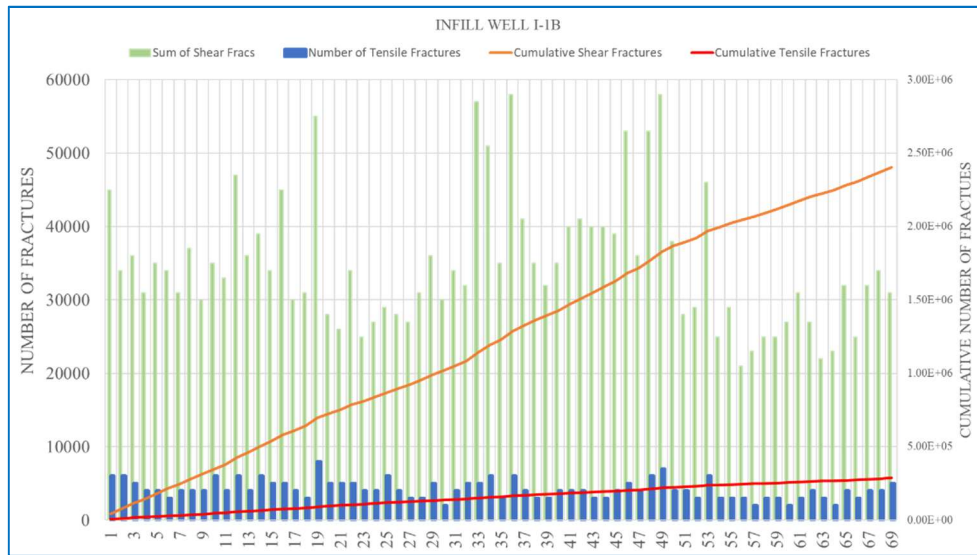


Figure 12–Shear and tensile fractures in infill Well I-1B

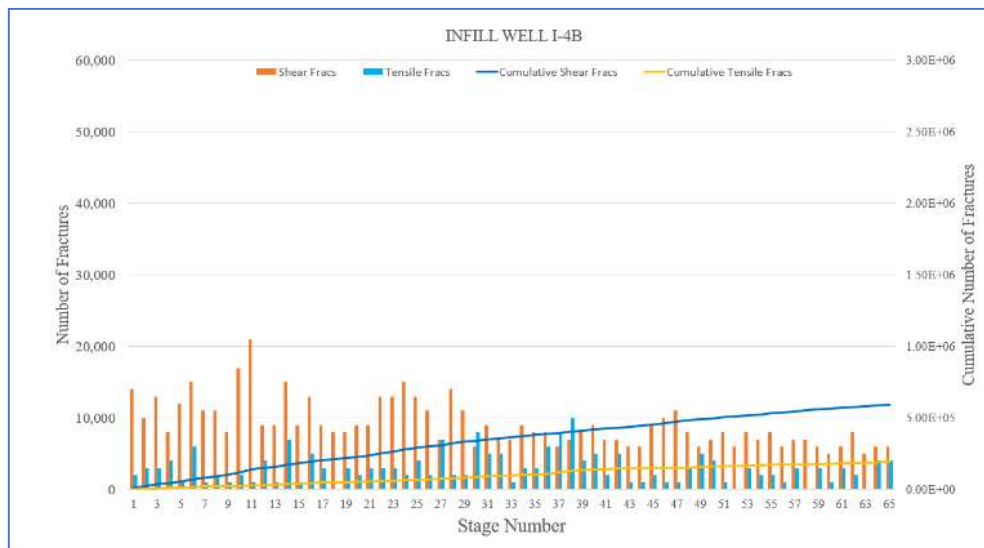


Figure 13–Fracture identification in Infill Well I-4B

Comparative Results

To confirm that the number of shear fractures and the VFR were correlative to well performance, RTA was used to evaluate the primary and infill wells. **FIGURE 14** shows the relative differences among the wells' LFP ($A_c\sqrt{k}$). We set the comparative well as the P1B primary well because we wanted to see the amount of deterioration from the primary well location. The percent shown is the LFP variance from the P1B. For the infill well I-1B, the LFP was 4% greater than the P1B and as good or better than its co-developed infills.

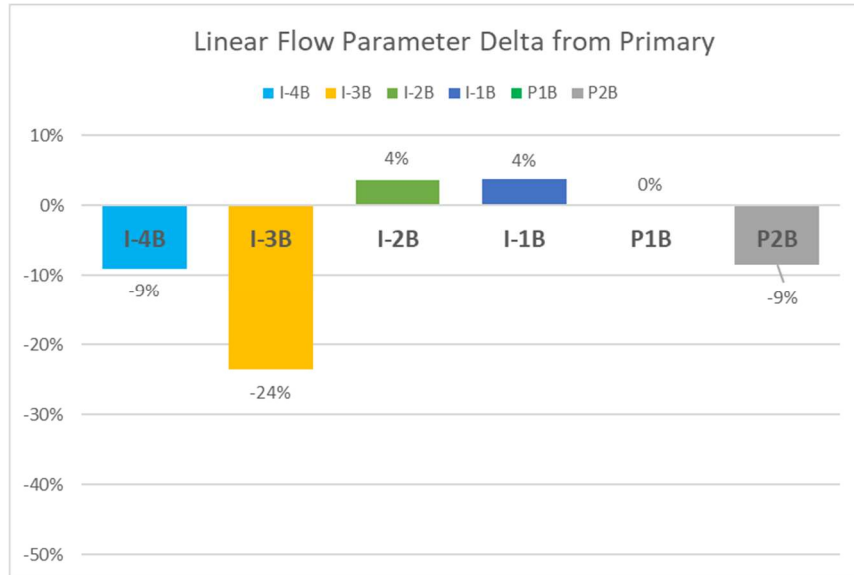


Figure 14–RTA Linear flow parameter differences from first order primary well

A comparison of the number of tensile fractures to the total fractures generated is shown in **FIGURE 15**. The percent of tensile fractures in the I-4B is more than double the first order infill I-1B. This correlates to the LFP however, we expected the I-3B to have greater percent tensile fractures correlative to the RTA. Typically, a bounded well like the I-3B, will have a smaller SRV due to fracture growth containment from its astride neighbor wells. To mitigate this potential, the I-3B had an additional 20% proppant loading which may have led to the higher number of shear to tensile fractures. We have not run a fracture analysis in the I-2B in time for this writing.

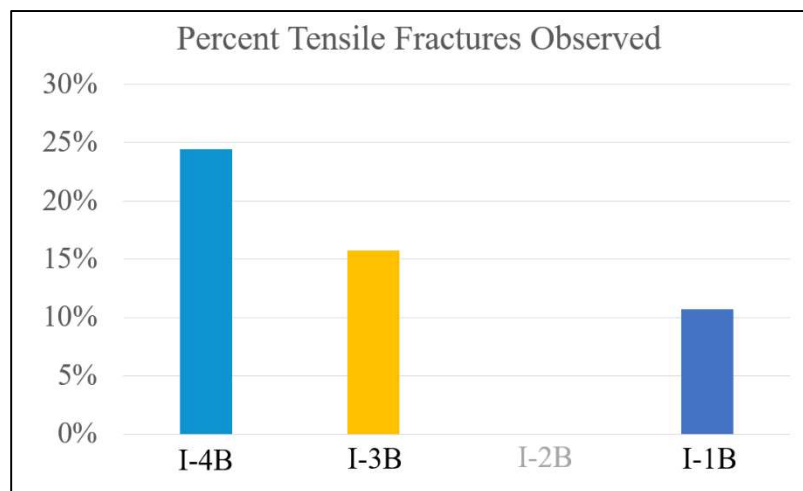


Figure 15–Percent tensile fractures observed in infill wells

A visual comparison was made of VFR and Shear Fractures shown in **FIGURE 16**. We previously established that VFR was inversely correlated to FDI magnitude (Figure 9). In the stages with frac to frac magnitude FDI, stages 33 and onward (highlighted by the box in Fig. 16) there is a compelling relationship between the amount of shear fractures and the VFR. In the heel area from stages 50 onward the VFR follows the shear fracture count. Although the VFR in this region (stages 50-65) is lower, the relationship implies that if the shear fracture count could be increased, the VFR (fracture efficiency) would be increased.

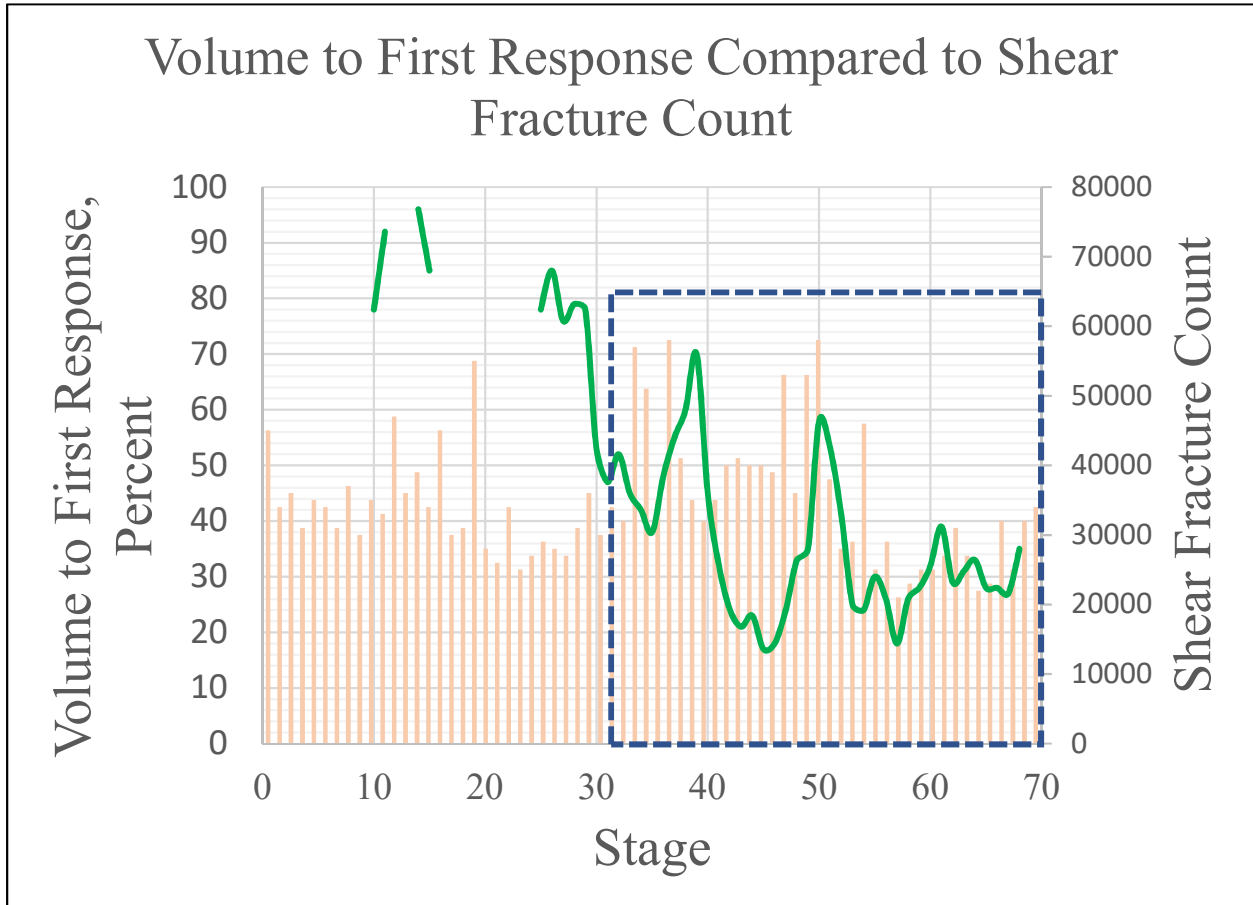


Figure 16–VFR compared to shear fracture count

The team also found correlations between the number of tensile fractures and FDIs. In **FIGURE 17** we compared the tensile fracture count per stage with the VFR in the corresponding stage. A box highlights the stages in Fig. 17 where we previously confirmed FDIs (Figure 8), in stages 33 onward. Using the VFR as a proxy for FDIs (low VFR equates to a fracture to fracture FDI), we found an inverse relationship of tensile fractures and VFR. For example, in stage 39 with a lower tensile frac count, the VFR increased to 70%. Conversely in stages 45 to 47, with the lowest VFR and highest FDI magnitude, the tensile fracture count is higher.

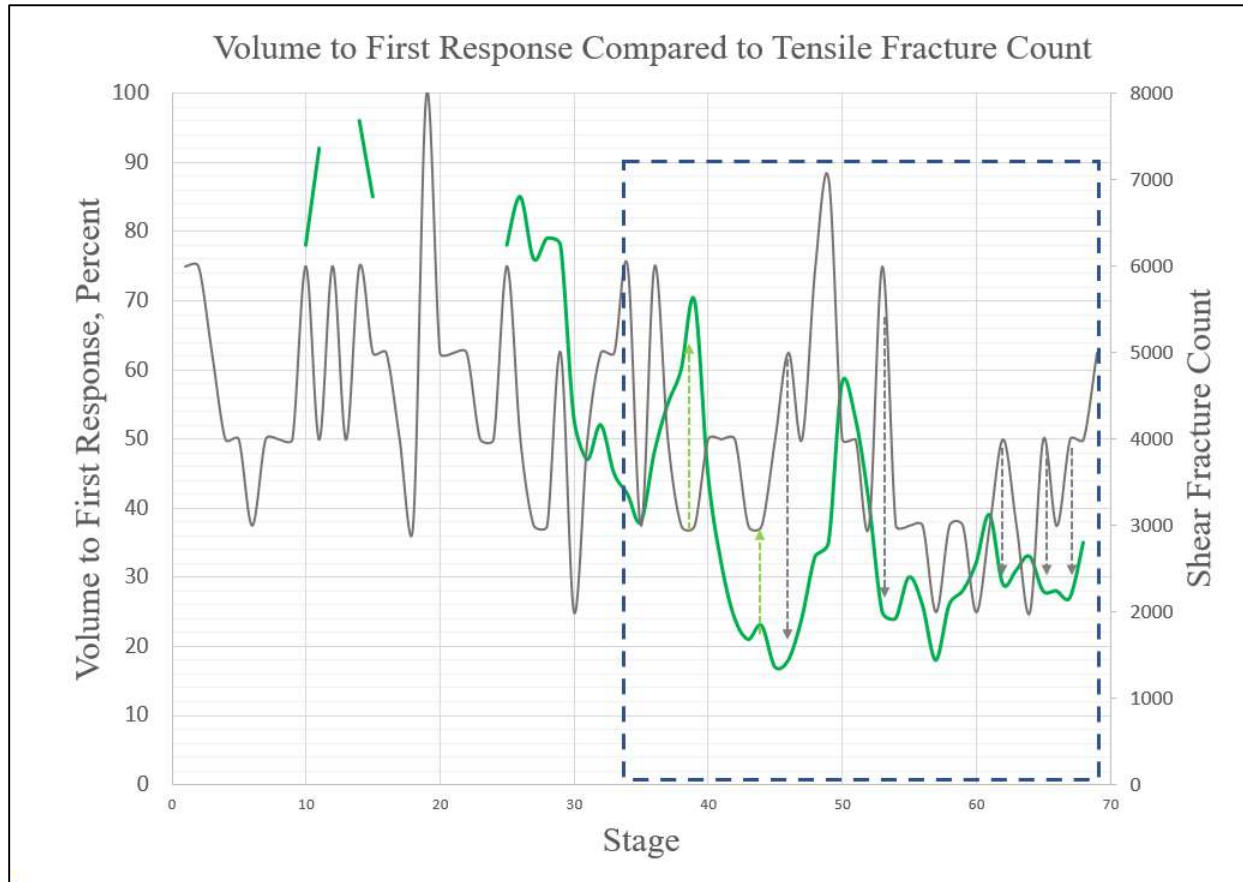


Figure 17–VFR compared to tensile fracture count

Fracture type identification was used in conjunction with other diagnostic tools to holistically assess the first order infill well. The tensile numbers show potential cause of an FDI; however, in stages 1 to 33 there were many instances of high number of tensile fractures, yet these did not cause the frac to frac communication observed in stages 40 onward. We observed that as the stages progressed, the event to FDI time (Figure 9) decreased substantially at stage 29 from 70 to 50 minutes. The FDI magnitude at this point was considered a stress shadow, under 20 psi. Increasing stress in the wellbore shown in the ISIP plot (Figure 10) resulted in fracture to fracture connections at stages 40 and onward. From stage 40, the increased stress made the primary well vulnerable to tensile fractures from the active well.

Discussion

The first order infill I-1B is either comparable or outperforming the initially unconstrained primary wells. In this paper we detail the Middle Wolfcamp wells, but we want to note that the linear flow parameter (LFP) among the Upper Wolfcamp infill wells are between 60%-100% of the primary wells. The lowest LFP is in the I-2A (Figure 11) not the first order infill; so, we believe the pre-loading may have positively affected the first order infill I-1A. However, we have not done the in-depth analysis of this bench. The LFPs suggest that the Middle Wolfcamp had better success with pre-loading than the shallower Upper Wolfcamp interval.

The RTA observations of LFP correlate with the independent measurements for number of shear fractures and VFR. Number of shear fractures were low for well I-4B and both the number of shear fractures and VFR were high for well I-1B. Comparatively, the LFP was low for I-4B, but high for I-1B. These results suggest that fracture surface area can be measured from the wellhead pressure every second and that VFR is a good measurement of total FSA created per stage.

It is important to note that the primary wells for both intervals were landed in slightly different landing depths compared to the infills, in that the first order primary was shallower and the second order was deeper (Fig 11). Given similar primary-infill well configurations for both intervals, using RTA to decide which set of wells within the interval had better success with passive frac mitigation is acceptable.

In summary, pre-loading the primary wells resulted in a more productive infill well in the Middle Wolfcamp interval. The VFR of the first order infill showed that most of the frac fluid stayed near the wellbore activating network fractures. A patented algorithm software confirmed the high number of shear fractures, and hence FSA, and RTA confirmed the findings of the fracture-type characterization.

Conclusions

The team found correlations between the wells' VFR, number of shear fractures, location where the FDIs occurred during the fracture treatment, and the infill well production performance. For instance, the VFR changes toward the heel stages is a telltale sign of reducing fracture efficiency, frac to frac connections, and resulting fracture asymmetry. RTA results show that the infill wells' SRV was like other co-developed infills if not better. The trial proved that pre-loading successfully may mitigate the predicted infill production degradation from depleted fractures in the primary well. Pre-loading likely aided the infill by providing a pressure barrier that helped keep the frac fluid in the infill hereby maximizing fracture surface area. Although we have not done the in-depth analysis in the Upper Wolfcamp wells, RTA suggests that the trial was more successful in the Middle Wolfcamp.

Incorporating new diagnostic tools such as VFR to evaluate fracture mitigation techniques provides a quantitative measure of determining success. As effective as these tools are, they are usually deployed in a lookback analysis like this study. Therefore, if a trial is successful, it is not known until weeks later.

The results in this study confirm that the patented algorithm software measuring the number and types of fractures does indeed indicate the effectiveness of the frac treatment as measured by "lookback" VFR and RTA. The advantage of the frac-type characterization is that it can be done "on the fly" giving the frac crew immediate feedback of the effectiveness of any operations change such as slowing the pump rate, adding more sand, or adding different chemicals. To enable completion engineers to create the maximum fracture surface area for the best producing wells, they must understand how to create shear fractures most

effectively within unconventional reservoirs. Unconventional reservoirs vary both stratigraphically and laterally, therefore real-time feedback during completion operations is the only way to understand and improve completion effectiveness per stage. The measurement of fractures every second is just one small, but essential part in what must be a holistic view when developing unconventional reservoirs.

Acknowledgements

We want to thank Endeavor Energy Resources for their continued support of industry collaboration by allowing us to publish this study.

We also want to thank Abra Controls and Shear FRAC for their important technical input and support of our efforts.

References

- Bommer, P., Bayne, M., Mayerhofer, M., Machovoe, M., & Staron, M. (2017, January 24). ReDesigning from Scratch and Defending Offset Wells: Case Study of a Six-Well Bakken Zipper Project, McKenzie County, ND. Society of Petroleum Engineers. doi: 10.2118/184851-MS
- Bommer, P. A., & Bayne, M. A. (2018, January 23). Active Well Defense in the Bakken: Case Study of a Ten-Well Frac Defense Project, McKenzie County, ND. Society of Petroleum Engineers. doi: 10.2118/189860-MS
- Couples, G. D. (2019). Where is the Water? - A Physical Analysis of Hydraulic Fracturing Processes. *AAPG ACE 2019*. San Antonio.
- Daneshy, A. (2018, September 17). Analysis of Horizontal Well Fracture Interactions, and Completion Steps for Reducing the Resulting Production Interference. Society of Petroleum Engineers. doi: 10.2118/191671-MS SPE-199686-MS 7
- Gross, M. R., Fischer, M. P., Engelder, T., & Greenfield, R. J. (1995). Factors controlling joint spacing in interbedded sedimentary rocks: integrating numerical models with field observations from the Monterey Formation, USA. *Geological Society Special Publication No. 92*, 215-233.
- Haustveit, K., Elliott, B., Haffener, J., Ketter, C., O'Brien, J., Almasoodi, M., . . . Sharma, S. (2020). Monitoring the Pulse of a Well through Sealed Wellbore Pressure Monitoring, a Breakthrough Diagnostic with a Multi-Basin Case Study. *SPE Hydraulic Fracturing Conference and Exhibition*. Houston: SPE-199731-MS.
- Haustveit, K., Almasoodi, M., Al-Tailji, W., Mukherjee, S., Palisch, T., & Barber, R. (2019, July 31). Far-Field Proppant Imaging Offsetting Depletion: A STACK Case History. Unconventional Resources Technology Conference. doi:10.15530/urtec-2019-1035
- Jacobs, T. (2019). To "Right Size" Fractures, Producers Adopt Robust Monitoring and Custom Completions. *Journal of Petroleum Technology*.
- Johnson, W. W. (2019). *United States of America Patent Application No. 16/190,088*.

King, G. E., Rainbolt, M. F., & Swanson, C. (2017, October 9). Frac Hit Induced Production Losses: Evaluating Root Causes, Damage Location, Possible Prevention Methods and Success of Remedial Treatments. Society of Petroleum Engineers. doi: 10.2118/187192-MS

Rainbolt, M. F., & Esco, J. (2018, January 23). Frac Hit Induced Production Losses: Evaluating Root Causes, Damage Location, Possible Prevention Methods and Success of Remediation Treatments, Part II. Society of Petroleum Engineers. doi: 10.2118/189853-MS

Scherz, R. Y., Rainbolt, M. F., Pradhan, Y., & Tian, W. (2019, January 29). Evaluating the Impact of Frac Communication Between Parent, Child, and Vertical Wells in the Midland Basin Lower Spraberry and Wolfcamp Reservoirs. Society of Petroleum Engineers. doi: 10.2118/194349-MS

Scherz, P. E., R. Y., Pradhan, P. E., Y., & Rainbolt, P. E., M. F. (2020, January 28). Mitigation for Fracture Driven Interaction: A Midland Basin Case Study. Society of Petroleum Engineers. doi:10.2118/199686-MS

Suarez-Rivera, R., Burghardt, J., Stanchits, S., Edelman, E., & Surdi, A. (2013). Understanding the Effect of Rock Fabric on Fracture Complexity for Improving Completion Design and Well Performance. *International Petroleum Technology Conference*.

Whitfield, T., Watkins, M. H., & Dickinson, L. J. (2018, September 17). Pre-Loads: Successful Mitigation of Damaging Frac Hits in the Eagle Ford. Society of Petroleum Engineers. doi: 10.2118/191712-MS